Letters

Characterization of a Nonlinear Resistive Polymer-Nanoparticle Composite Coating for Electric Field Reduction in a Medium-Voltage Power Module

Zichen Zhang, *Student Member, IEEE*, Khai D. T. Ngo, *Fellow, IEEE*, and Guo-Quan Lu, *Fellow, IEEE*

***Abstract*—Medium-voltage (MV) silicon carbide power devices are emerging and have the potential to serve in various power grid applications. However, the high blocking voltage and reduced size of the power modules require innovative insulation solutions. In this letter, a nonlinear resistive polymer-nanoparticle composite coating was characterized and, for the first time, demonstrated for reducing the high electric field at the triple point on a patterned substrate of a typical MV power module. The electrical properties of the coating were measured. Its conductivity showed nonlinear dependency on the applied electric field. The coating, which is about 20 μm thick, was applied along the triple-point edges on a patterned direct-bonded copper substrate. The partial discharge inception voltages of the coated substrates were measured in a transformer oil or in a silicone gel. The average increases in the inception voltage compared to the substrates without the coating were over 85% in the silicone gel. The increase agreed with the results of field simulations, which showed a 53% reduction of the maximum field in the silicone gel for a coated substrate. The processing simplicity and effectiveness of the coating present a cost-effective solution for insulating high-power-density, MV power modules.**

***Index Terms*—E-field reduction, medium-voltage (MV) power module, module insulation, nonlinear resistive polymer-nanoparticle composite, partial discharge inception voltage.**

I. Introduction

EMERGING medium-voltage (MV) silicon carbide (SiC) device technologies offer the opportunity to reduce the complexity and increase the efficiency of power electronics in various power-grid applications [1]–[3]. However, before the MV devices can be widely adopted, innovative solutions for their packaging, especially their insulation, are needed. With their reduced size and increased voltage rating, the insulation materials in the power modules, such as the insulated metal substrate and the encapsulant, are under much higher electric field (E-field) intensities. This can lead to dielectric failure or partial discharge (PD) that reduce the lifetime of the module. One way to increase the partial discharge inception voltage (PDIV) of the module is to increase the insulation thickness of the substrate. Even though this approach reduces the nominal E-field strength, the nonuniformity of the field will increase, making it a less effective solution [4]. Stacked substrates were proposed to shape the E-field and proved to be more effective in field reduction [5]. However, both the substrate-thickening and substrate-stacking approaches increase the module's thermal resistance. Given that the MV wide-bandgap devices are expected to handle higher heat fluxes because of their higher-rated current densities than their silicon counterparts [6], an insulation solution that trades off thermal performance for meeting the insulation requirement is not ideal.

Material solutions for improving module insulation have also been explored [7]–[11]. Capacitive field materials were widely studied. However, their high viscosity [7], high power loss [7], and complicated material processing [8] make them difficult to apply to a real MV power module. Nonlinear resistive materials were suggested in [9]–[11] and are preferred for power modules under pulsewidth modulation (PWM) excitations. Compared to linear semiconducting or conductive materials, nonlinear resistive materials offer a balance between power loss and E-field reduction due to their field-dependent behavior. Auspicious E-field simulation results were reported in [11]. However, to date, there has not been any experimental demonstration of a nonlinear resistive field-grading material in power modules. Recently, we completed a simulation study to find the desired properties of a nonlinear resistive material for reducing the E-field intensities at the triple-point (TP) edges on a direct-bonded copper (DBC) substrate [12]. The letter was aimed at providing a guideline for materials engineers to develop effective field-reduction materials.

In this letter, the electrical properties of a nonlinear resistive polymer-nanoparticle composite were characterized and its effectiveness for increasing the PDIV of a patterned DBC substrate was demonstrated. The dielectric constant and electrical conductivity of the coating were measured. The coating was applied along the TP edges on the patterned DBC substrate. The PDIVs of the coated and uncoated substrates were measured in a transformer oil or encapsulated by a silicone gel. Using the

Manuscript received July 15, 2021; revised August 12, 2021; accepted September 6, 2021. Date of publication September 13, 2021; date of current version November 30, 2021. This work was supported by the Advanced Research Projects Agency-Energy of the Department of Energy under Grant DE-AR0001008. *(Corresponding author: Guo-Quan Lu.)*

Zichen Zhang and Khai D. T. Ngo are with the Bradley Department of Electrical and Computer Engineering, Center for Power Electronics Systems, Virginia Tech, Blacksburg, VA 24061 USA (e-mail: zichen2013@vt.edu; kdtn@vt.edu).

Guo-Quan Lu is with the Department of Materials Science and Engineering, Virginia Tech, Blacksburg, VA 24061 USA, and also with the Bradley Department of Electrical and Computer Engineering, Center for Power Electronics Systems, Virginia Tech, Blacksburg, VA 24061 USA (e-mail: gqlu@vt.edu).

Color versions of one or more figures in this article are available at https://doi.org/10.1109/TPEL.2021.3112096.

Digital Object Identifier 10.1109/TPEL.2021.3112096

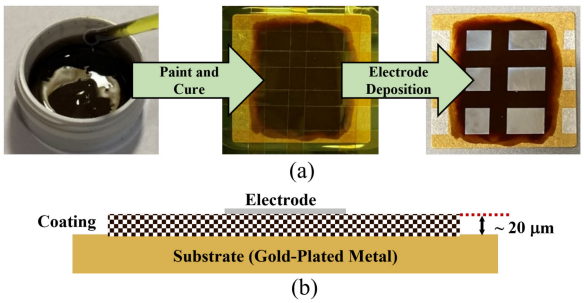

Fig. 1. (a) Process flow for preparing the coating samples for electrical characterization. (b) Schematic of the cross section of a coating sample.

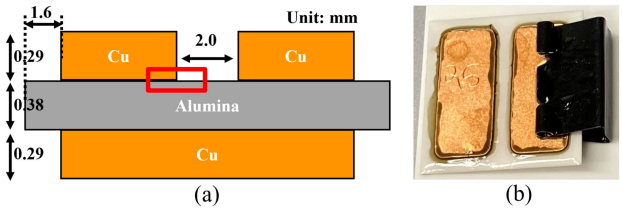

Fig. 2. (a) Schematic of the DBC test coupon. (b) Photo of a coated DBC sample after silicone encapsulation.

measured electrical properties of the coating and the geometry of the coated DBC substrate, a field simulation was run to find the reduction of the maximum E-field intensity in the coated substrate. Agreement was found between the measured increase in PDIV and the simulated field reduction.

II. Experimental Procedure

A. Electrical Property Characterization of the Coating

A nonlinear resistive polymer-nanoparticle composite solution under the trade name of nanoEshield was acquired from NBE Technologies, LLC, Blacksburg, VA, USA. The solution is a mixture of inorganic nanoparticles, a polymer, and an organic solvent. The viscosity of the solution was about 20 000 cps, and it was printable by a paintbrush. The recommended curing profile to form a coating was 140 °C for 30 min. According to its supplier, the glass transition temperature of the coating is about 120 °C, and its decomposition temperature is about 200 °C. These thermal characteristics are similar to those of a typical electronic epoxy encapsulant. We were also told that the bonding strength of the coating on copper or on alumina is around 5 MPa. This is sufficient for a thin, soft polymeric coating serving as an intermediate between a hard material and a softer material like a silicone gel. To characterize the dielectric constant and conductivity of the coating, thin film samples were prepared on a smooth electrically conductive substrate. Shown in Fig. 1(a) are: the as-received composite solution; a coating formed on a gold surface-finish substrate; and an electrical test sample with multiple silver electrodes deposited by E-beam evaporation on the coating.

A probe station was used to measure the *I–V* and *C–V* characteristics of the coating. Considering the region under a deposited electrode in Fig. 1(b), the conductivity σ and dielectric constant ε_r can be calculated by

$$\sigma = \frac{I}{V}\frac{t}{A}, \text{ and} \tag{1}$$

$$\varepsilon_r = \frac{C}{\varepsilon_0}\frac{t}{A} \tag{2}$$

where ε_0 is the vacuum permittivity, the area A was measured under an optical microscope, the coating thickness t was measured by a DEKTAK stylus profilometer, V is the applied voltage between the deposited electrode and the metal substrate, and the current I and the capacitance C were measured by the probe station.

B. PDIV Measurements of Coated Substrates

To evaluate the effectiveness of the coating on field reduction, samples of a 21 mm × 21 smm alumina DBC substrate, with other dimensions detailed in Fig. 2(a), were prepared. The copper (Cu) pattern on one side of the substrate was chemically etched. The 2 mm trench gap is typical for electrical isolation in MV power modules. The coating was applied along the Cu edges on both sides of the substrate. Fig. 2(b) shows a sample after the Cu edges of the patterned side were coated and covered by a silicone gel. The black metal clamp in the figure was used to short the back of the DBC to one of the top electrodes. For PDIV measurements, the samples were either submerged in a transformer oil or encapsulated by a silicone gel such as the one shown in Fig. 2(b). The isolated Cu trace would be connected to a PD-free high-voltage 60 Hz ac source, while the other electrode and the bottom Cu would be grounded. According to [13], this electrical excitation would produce the worst-case electric field distribution in the insulation materials. Abiding by the standards set forth by the IEC 60270, the PD threshold level was set at 10 pC, and the PDIV was monitored by a PD detection system (MPD-600). The PDIV of a sample in oil was first measured. Then the sample was thoroughly cleaned to remove the grease and was retested for PDIVs. For comparison, PDIVs of samples without the coating were also measured.

C. Cross-Sectional View of Coated DBC Substrate

To determine the extent of the coating along the Cu edges, a sample was potted in an epoxy, polished, and lapped for cross-section imaging. Fig. 3(a) shows an edge view of a sample bonded in epoxy before polishing. It was polished down with a SiC sandpaper to a region of interest. Then, the sample was lapped to surface roughness below 100 nm on an auto polisher with alumina suspensions. Fig. 3(b) shows the TP at the Cu electrode edge surrounded by the DBC alumina and with the coating at 15 to 30 μm thick. Chemical etching of the electrode left a sharp corner at the TP.

III. Results and Discussion

A. Coating Electrical Properties

Figs. 4(a) and (b) show the measured *C–V* and *I–V* curves of the coating, respectively. The capacitance was measured under a peak ac bias of 25 mV at 100 kHz on top of a dc bias that

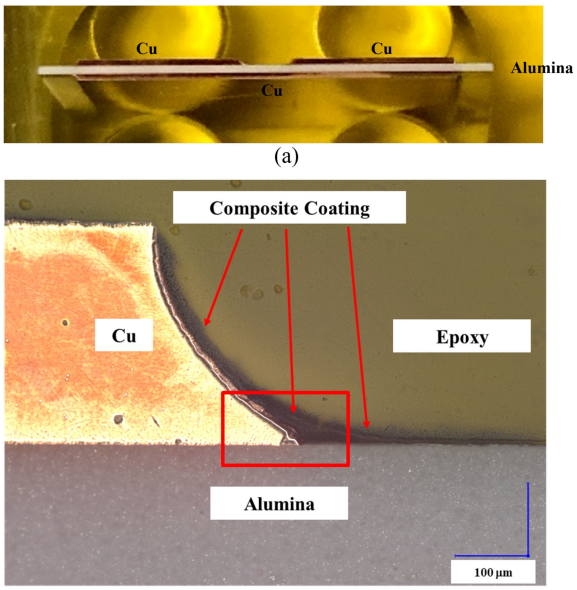

Fig. 3. (a) Edge view of a coated sample bonded in an epoxy for cross-section imaging. (b) Optical image of the TP of the sample after polishing and lapping. The various materials surrounding the TP are labeled in the figure.

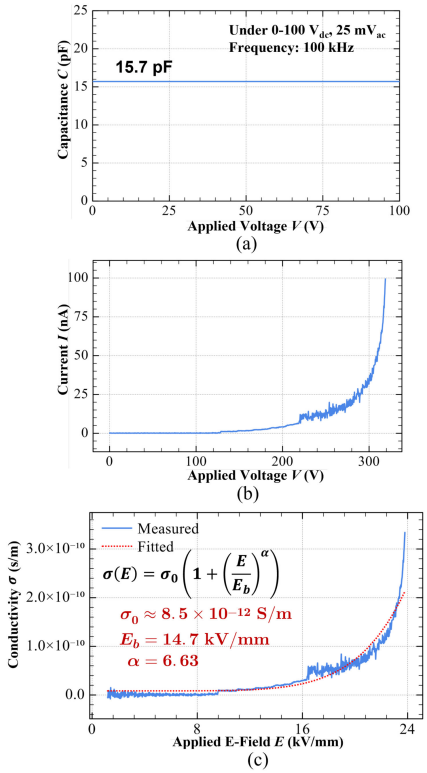

Fig. 4. (a) Measured C–V curve on a sample under 25 mV ac at 100 kHz on dc voltages from 0 to 100 V. (b) Measured I–V curve of the same sample. (c) Calculated and fitted conductivity versus average E-field from (b) and (3).

varied from 0 to 100 V. The capacitance of the coating was found to be independent of the applied dc voltage. From (2), the dielectric constants of different coating samples were calculated and ranged from 2.2 to 4.5 because of variations in coating thickness and microstructure. The I–V curve showed non-ohmic behavior, or nonlinear behavior, which is necessary for grading the E-field [10]. From (1) and Fig. 4(b), the conductivity of the coating was calculated as a function of the average E-field intensity, as plotted in Fig. 4(c). Equation (3) from [9] was used to fit the measured conductivity versus E-field curve

$$\sigma\ (E) = \sigma_0 \left(1 + \left(\frac{E}{E_b}\right)^{\alpha}\right) \tag{3}$$

where σ_0, E_b, and α are the low-field conductivity, switching field, and nonlinear coefficient, respectively. In Fig. 4(c), (3) with the fitted parameters is plotted on the measured curve, showing a reasonably good match.

B. PDIV Results

Shown in Fig. 5(a) are the PDIVs measured from coated and uncoated DBC substrates submerged in the oil. The coating improved the substrate PDIV by about 30%. Shown in Fig. 5(b) are the PDIVs measured from coated and uncoated samples encapsulated in the silicone gel. In this case, the coating improved the substrate PDIV by 85 to 100%. It is notable that the average PDIV of the uncoated samples submerged in the oil was significantly higher, by about 40%, than that of the uncoated samples encapsulated in the gel. Since the silicone gel had a much higher viscosity than the oil, it is likely that the gel-encapsulated samples had trapped air bubbles along the TP edges, thus reducing their PDIVs.

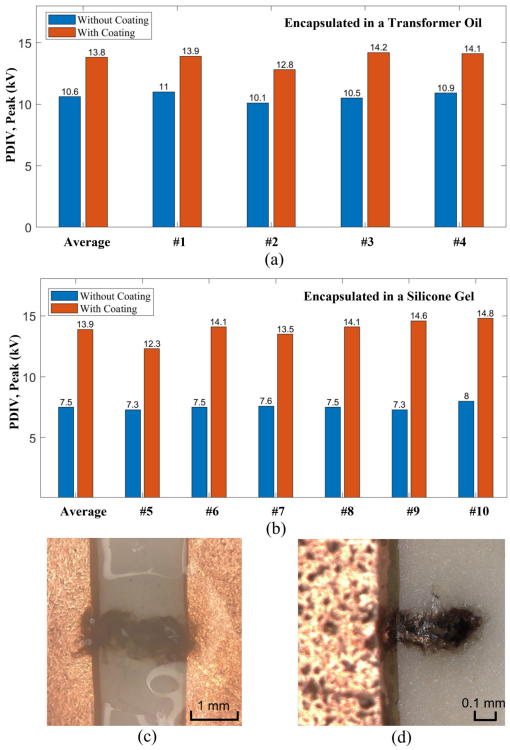

Fig. 5. (a) PDIVs of the DBC samples with and without the coating measured in the oil. (b) PDIVs of the DBC samples with and without the coating measured with the silicone gel encapsulation. (c) Photo of a burnt trench in an uncoated and silicone-encapsulated sample. (d) Photo of a burnt trench in a coated and silicone-encapsulated sample.

TABLE I
MATERIAL PROPERTIES USED IN THE E-FIELD SIMULATION

	Material Property	Simulated Value
Alumina	Dielectric Constant	9.9
	Conductivity	10^{-12} S/m
Silicone Gel	Dielectric Constant	2.7
	Conductivity	10^{-13} S/m
Field-Grading Coating	Dielectric Constant	4
	Low-Field Conductivity	10^{-11} S/m
	Switching Field	15 kV/mm
	Nonlinear Coefficient	7

For some samples encapsulated in the gel, their breakdown voltages were also measured. The breakdown voltage of an uncoated sample was about 8.0 kV, and that of a coated sample was about 15.0 kV. Fig. 5(c) and (d) show the dielectric breakdown sites on an uncoated and a coated sample, respectively. Without the coating, the breakdown started inside the silicone gel at the gel-alumina interface. However, with the coating, there was a crack or cavity in the alumina, suggesting that the silicone gel was not the weakest insulator. This may explain why the coated samples, whether measured in the oil or in the gel, all had about the same PDIV: the coating significantly reduced the E-field strength in gel, making the alumina the weakest insulator. The following section provides support from E-field simulations of the trench.

C. E-Field Simulations and Discussion

In [12], the effects of a nonlinear resistive coating at the TP on E-field distribution were simulated using hypothetical electrical properties of the coating and coated geometry. With the measured properties and coating/TP geometry, field simulations were run again to find the reduction of the maximum field strength in the gel. The E-field simulation model was constructed in COMSOL. The applied voltage across the Cu electrodes was a sinusoidal function with a 15-kV amplitude. One of the two Cu electrodes was grounded in the same way as in the PDIV test. All the material properties used in the simulations are listed in Table I. Fig. 6(a) is a plot of the simulated field distribution around the TP in the trench without the coating, and Fig. 6(b) is the distribution with the coating. The distributions were taken at $t = 0.005$ s when the applied voltage was at its maximum. From the field maps, the coating clearly reduces the field intensities in both the alumina and the gel around the TP. The ratio of the maximum field intensities in the gel with and without the coating was found by following the methodology in [14] to determine the field intensities by avoiding singularity at the TP. A dotted line, L, generally called the measure line, was drawn across the TP at 15 μm above and parallel to the surface of the alumina. E-field intensities along this line were measured and plotted.

Plotted in Fig. 6(c) are the field intensities along the measure line across the TP in the trench with and without the coating. The coating moved the maximum E-field intensity in the gel from Point A, the electrode-gel boundary, to Point B, the coating-gel boundary, and reduced the maximum intensity by 53%. This

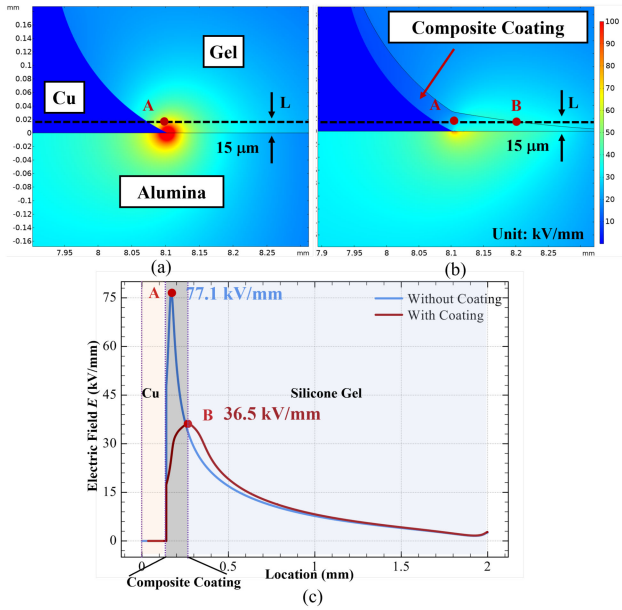

Fig. 6. Simulated E-field distributions around the triple point in the trench (a) without coating, (b) with coating, and (c) along the measure line L from (a) and (b). The material boundaries along L, Points A and B, are labeled accordingly.

field reduction would correspond to an increase in PDIV of 127%, which is in good agreement with the 85%–100% PDIV increases measured in the coated over uncoated samples.

A detailed explanation for our observations can be found in [9]–[11]. To put it simply, as the conductivity of the nonlinear resistive coating increases under high applied field, space charges develop across the coating. The electric field by the space charges counters the applied field, lowering the field intensities around the triple point and leading to a higher PDIV. There might be another reason for the significant PDIV increase. The coating might be more affinitive to the electrode, the substrate, and the gel than the gel to the electrode and the substrate. If this is the case, the coating could reduce the probability of air bubbles formed at the triple point and/or the likelihood of PD along the various material interfaces. More studies are needed to sort out the latter hypothesis.

IV. CONCLUSION

A polymer-nanoparticle composite material was characterized as a field-reduction coating of the triple point on an MV power module substrate. The dielectric constant of the coating was found to be about 3.0, and its electrical conductivity showed nonlinear dependence on the E-field intensity with a switching field at around 15 kV/mm. Patterned DBC substrates with their triple points along the edges of the electrodes were coated by about 20 μm thick of the material, and their PDIVs were measured in a transformer oil or in a silicone gel. The coating increased the PDIVs of the substrates by over 30% measured in the oil or by over 85% in the gel. The E-field distributions around the triple point on the substrate were simulated with and without the coating. The significant increases in PDIVs of the coated substrates obtained in the gel were found to be in good agreement with the reduction of the maximum E-field intensity

in the gel. Our findings offered an experimental validation of a practical nonlinear resistive material for E-field grading in MV power modules.

ACKNOWLEDGMENT

The authors would like to thank C. Nicolas at Virginia Tech for help with the PDIV measurements and NBE Technologies for providing the polymer-nanoparticle composite solution.

REFERENCES

[1] A. Jafari *et al.*, "Comparison of wide-band-gap technologies for soft-switching losses at high frequencies," *IEEE Trans. Power Electron.*, vol. 35, no. 12, pp. 12595–12600, Dec. 2020.

[2] S. Ji, Z. Zhang, and F. Wang, "Overview of high voltage SiC power semiconductor devices: Development and application," *CES Trans. Electr. Mach. Syst.*, vol. 1, no. 3, pp. 254–264, 2017.

[3] B. Passmore and C. O'Neal, "High-voltage SiC power modules for 10-25 kV applications," *Power Electron. Europe Mag.*, no. 1, pp. 22–24, 2016. [Online]. Avalaible: https://www.power-mag.com/pdf/feature_pdf/1461163294_Woifspeed_Feature.pdf

[4] U. Waltrich, C. Bayer, M. Reger, A. Meyer, X. Tang, and A. Schletz, "Enhancement of the partial discharge inception voltage of ceramic substrates for power modules by trench coating," in *Proc. Int. Conf. Electron. Packag.*, 2016, pp. 536–541.

[5] O. Hohlfeld, R. Bayerer, T. Hunger, and H. Hartung, "Stacked substrates for high voltage applications," in *Proc. 7th Int. Conf. Integr. Power Electron. Syst.*, 2012, pp. 1–4.

[6] B. J. Baliga, *Fundamentals of Power Semiconductor Devices*. Berlin, Germany: Springer, 2010.

[7] N. Wang, I. Cotton, J. Robertson, S. Follmann, K. Evans, and D. Newcombe, "Partial discharge control in a power electronic module using high permittivity non-linear dielectrics," *IEEE Trans. Dielectr. Electr. Insul.*, vol. 17, no. 4, pp. 1319–1326, Aug. 2010.

[8] S. Diaham, Z. Valdez-Nava, T. Le, L. Lévêque, L. Laudebat, and T. Lebey, "Field grading composites tailored by electrophoresis—Part 3: Application to power electronics modules encapsulation," *IEEE Trans. Dielectr. Electr. Insul.*, vol. 28, no. 2, pp. 348–354, Apr. 2021.

[9] T. Christen, L. Donzel, and F. Greuter, "Nonlinear resistive electric field grading part 1: Theory and simulation," *IEEE Electr. Insul. Mag.*, vol. 26, no. 6, pp. 47–59, Dec. 2010.

[10] L. Donzel, F. Greuter, and T. Christen, "Nonlinear resistive electric field grading Part 2: Materials and applications," *IEEE Electr. Insul. Mag.*, vol. 27, no. 2, pp. 18–29, Apr. 2011.

[11] L. Donzel and J. Schuderer, "Nonlinear resistive electric field control for power electronic modules," *IEEE Trans. Dielectr. Electr. Insul.*, vol. 19, no. 3, pp. 955–959, Jun. 2012.

[12] J. Xu, Z. Zhang, K. Ngo, and G.-Q. Lu, "Desired properties of a nonlinear resistive coating for shielding triple point in a medium-voltage power module," *IEEE Trans. Dielectr. Electr. Insul.*, 2021, doi: 10.1109/TDEI.2021.009507.

[13] Z. Zhang *et al.*, "Packaging of an 8-kV silicon carbide diode module with double-side cooling and sintered-silver joints," in *Proc. IEEE Electr. Ship Technol. Sympo.*, 2021, pp. 1–7.

[14] C. Bayer, E. Baer, U. Waltrich, D. Malipaard, and A. Schletz, "Simulation of the electric field strength in the vicinity of metallization edges on dielectric substrates," *IEEE Trans. Dielectr. Electr. Insul.*, vol. 22, no. 1, pp. 257–265, Feb. 2015.